Structural Basis of the Tanford Transition of Bovine β-Lactoglobulin[†,‡]

Bin Y. Qin,[§] Maria C. Bewley,[||,⊥] Lawrence K. Creamer,[#] Heather M. Baker,[||,△] Edward N. Baker,*[,||,△] and Geoffrey B. Jameson*[,§]

Centre for Structural Biology, Institutes of Fundamental Sciences and Molecular Biosciences, Massey University, Palmerston North, New Zealand, and New Zealand Dairy Research Institute, Palmerston North, New Zealand

Received May 4, 1998; Revised Manuscript Received July 22, 1998

ABSTRACT: The structures of the trigonal crystal form of bovine β-lactoglobulin variant A at pH 6.2, 7.1, and 8.2 have been determined by X-ray diffraction methods at a resolution of 2.56, 2.24, and 2.49 Å, respectively. The corresponding values for R (R_{free}) are 0.192 (0.240), 0.234 (0.279), and 0.232 (0.277). The C and N termini as well as two disulfide bonds are clearly defined in these models. The glutamate side chain of residue 89 is buried at pH 6.2 and becomes exposed at pH 7.1 and 8.2. This conformational change, involving the loop 85−90, provides a structural basis for a variety of pH-dependent chemical, physical, and spectroscopic phenomena, collectively known as the Tanford transition.

Bovine β-lactoglobulin (BLG)[1] is the major whey protein of cow's milk with a concentration of 0.3 g/100 mL (*1*) and was first isolated in 1934 (*2*). This protein, which has 162 residues in its mature form, exists as a dimer in solution, where the dimer has a molecular weight of approximately 36 000 (*3*). BLG has a calyx fold, typical of the lipocalin protein superfamily (*4*), and shares with other lipocalins the ability to bind a variety of small hydrophobic molecules in vitro (*5*−*8*). β-Lactoglobulins are widely distributed. While some BLG's are monomeric, for example, horse (*9*), pig (*10*), and cat (*11*), most BLG's occur as dimers, especially, for example, in the order of hoofed mammals, *Artiodactyla* (*12*). The ruminant animals have dimeric BLG's, which show very high sequence identity to bovine BLG (*13*). Within a species, BLG often exists in several genetic variants. The cow (*Bos taurus*), for example, has at least nine variants, labeled as A, B, C, D, E (*14*), H (*15*), I, J (*16*), and W (*17*). The more common bovine BLG variants (A, B, and C) respond differently to heat, a property of technological significance in the industrial processing of milk and for the characteristics of milk products (*18*). Bovine BLG is stable at low pH (*19*), is resistant to proteolysis (*20*), and remains mostly intact after it passes through the stomach (*21*). Its concentration is particularly high during the colostral period of lactation (*22*). Even though a retinol−BLG complex receptor has been found in newborn calves (*23*), the real physiological function of BLG remains mysterious after more than 60 years of research. It has been suggested that BLG is involved in the digestion of milkfat and/or the transportation of retinol (*24*). Of nutritional significance is that human milk does not contain BLG (*25*).

Bovine BLG crystallizes in at least six crystal forms (*26*) and was the subject of X-ray diffraction investigations as early as 1938 (*3*). Low-resolution (6 Å) structures of BLG in lattices X (triclinic), Y (orthorhombic), and Z (trigonal) have existed for some time (*27*). A medium-resolution (2.8 Å) structure of BLG in lattice Y (*23*) identified a calyx fold similar to that of retinol-binding protein (RBP) (*28*) and now known to be typical of the lipocalin superfamily. High-resolution structures of BLG in lattices X (*29*) and Y (*30*) have been published recently, although both structures are reported to contain several ill-defined regions. The structure of BLG in lattices Y and Z, as originally determined (*23*, *31*), contained a number of out-of-register errors that have only recently been corrected in an analysis of BLG in lattice Z at 3 Å resolution (*29*), lattice X at 1.8 Å resolution (*29*), and lattice Y at 1.9 Å resolution (*30*).[2]

Here we present the structure of bovine BLG (pure variant A) in lattice Z at considerably higher resolution than previously reported (*29*). The higher resolution may arise because the material used in this study was pure variant A rather than a mixture of variants A and B, which differ at Asp64 (Gly in variant B) and at Val118 (Ala in variant B). More importantly, the structure of BLG has been determined at three different pH values (6.2, 7.1, and 8.2). For the first time it is possible to define a structural change that can account for the pH-dependent behavior of bovine BLG, free from potential complications of different crystal-packing effects (of different crystal forms) on the conformations of the flexible loops that plague the various structure analyses

[†] This work was supported in part by a grant from the New Zealand Dairy Research Institute, through a grant from FoRST of New Zealand (DRI 403).

[‡] PDB codes for the structures reported herein: BLGA at pH 6.2, 3blg; BLGA at pH 7.1, 1bsy; BLGA at 8.2, 2blg.

* To whom correspondence may be addressed (e-mail: Ted.Baker@auckland.ac.nz; G.B.Jameson@massey.ac.nz).

[§] Institute of Fundamental Sciences, Massey University.

[||] Institute of Molecular Biosciences, Massey University.

[⊥] Current address: Biology Department, Brookhaven National Laboratory, Upton, NY 11973.

[#] New Zealand Dairy Research Institute.

[△] Current address: School of Biological Sciences, Auckland University, Private Bag 92-019, Auckland, New Zealand.

[1] Abbreviations: BLG, β-lactoglobulin; BLGA, β-lactoglobulin variant A (similarly, variants B and C); HEPES, *N*-(2-hydroxyethyl)-piperazine-*N*′-2-ethanesulfonic acid; RMS, root mean square; SDS−PAGE, sodium dodecyl sulfate−polyacrylamide gel electrophoresis; TAPSO, 3-*N*-[tris(hydroxymethyl)methyl]-3-aminopropanesulfonic acid.

[2] Manuscript in preparation.

S0006-2960(98)01016-2 CCC: $15.00
Published on Web 09/18/1998

of BLG. Such pH-dependent behavior has been recognized for a long time. Centrifugation experiments by Pedersen in 1936 revealed that the sedimentation coefficients of BLG decreased with increasing pH in the range 6−8 (*32*). In 1951, Groves, Hipp, and McMeekin reported an increase in optical levorotation of BLG with increasing pH (*33*); this result was later extended to specific BLG variants (*34*). Tanford, Bunville, and Nozaki in 1959 found anomalous titration behavior for BLG (*35*) and proposed that this arose from a carboxyl group with a pK_a of 7.3, which was buried at acidic pH but became exposed at basic pH. More recently, pH-dependent changes in the thermal behavior of BLG were observed (*36*): a peak in the thermalgram present at pH 6.75 disappears at pH 8.05. Another pH-related phenomenon, described by Dunnill and Green (*37*), is that the free sulfhydryl group of BLG can react with reagents containing Hg^{2+} much more readily above pH 6.7. Collectively, those pH-dependent changes, which occur at pH ~7, in physical, chemical, and spectroscopic properties of BLG are known as the N ⇔ R or Tanford transition (*35*). Here, the anomalous carboxylate residue is identified as Glu89, as proposed by Brownlow et al. (*29*), and the structural transition is shown to involve a loop movement.

EXPERIMENTAL PROCEDURES

A sample of bovine β-lactoglobulin variant A (BLGA), isolated from the milk of a homozygous cow, was provided by the New Zealand Dairy Research Institute. The purity of the sample was confirmed by SDS−PAGE. BLGA at a protein concentration of 25−30 mg/mL in 0.010 M HEPES at pH 7.4 was subjected to an ammonium sulfate crystal screen. The screen matrix was 4 × 6, with six equally spaced concentrations of ammonium sulfate from 2.2 to 2.8 M, and four buffers at a concentration of 0.18 M with pH 5.0 (acetic acid/KOH), 6.1 (cacodylic acid/KOH), 7.4 (HEPES/KOH), and 8.7 (TAPSO/KOH). Crystals grew in hanging drops, comprising 2 μL of protein solution and 2 μL of well solution. The well solutions with nominal pH 6.1, 7.4, and 8.7, which produced the crystals suitable for data collection, have their pH shifted to 6.2, 7.1, and 8.2, respectively, by the ammonium sulfate. In general, BLGA will produce crystals in the lattice Z form in 2−4 days over an ammonium sulfate concentration range of 2.2−2.8 M.

X-ray diffraction data sets were collected at room temperature with a Rigaku RAxis IIC image plate detector and a Rigaku RU200 rotating anode generator. The data were processed and indexed by the program DENZO (*38*) and merged by the program SCALEPACK (*39*). Data collection statistics are summarized in Table 1. By means of the program AMoRe (*40*), the structure of BLGA at pH 8.2 in lattice Z was solved by molecular replacement methods, using as a search model the redetermined structure of BLGA from the orthorhombic crystal form (lattice Y) (*30*);[2] the mobile regions were excluded. The initial *R* factor was 0.43 for a model comprising residues 1−61, 66−110, and 116−152. The program X-PLOR (*41*) was used to refine the initial model, with the free *R* factor, R_{free} (*42*), used to monitor the progress of the refinement. Extensive rebuilding, using the molecular graphics program TURBO (*43*), was involved in the whole refinement procedure. The refined BLGA structure at pH 8.2 in lattice Z was used as the starting model to obtain the models for BLGA in lattice Z at pH 7.1 and 6.2. A set of ~550 reflections was separately and randomly chosen for calculations of R_{free} for each structure. Unit cell and intensity differences (R_{merge} = 0.27 for combining the three data sets) made these R_{free} sets reasonably independent, as shown by the similar starting *R* factor of ~0.4 for each structure. Simulated annealing (X-PLOR), to remove phase bias, gave inconsistent results. Limited refinement, therefore, preceded calculation of omit maps, and this procedure largely eliminated any bias. All structures have acceptable quality statistics, as analyzed by PROCHECK (*44*) and summarized in Table 2.

Table 1: Reflection Data Set Statistics of BLGA in Lattice Z

	pH 6.2	pH 7.1	pH 8.2
space group	$P3_22_1$	$P3_22_1$	$P3_22_1$
unit cell			
a (Å)	53.75	53.9	54.29
b (Å)	53.75	53.9	54.29
c (Å)	111.5	112.40	113.1
α (deg)	90	90	90
β (deg)	90	90	90
γ (deg)	120	120	120
unit cell volume (Å^3)	279111	283429	288901
lattice type code	Z	Z	Z
unique reflections	6422	9293	7203
last shell (Å)	2.61−2.56	2.28−2.24	2.51−2.46
redundancy	3.28	3.07	2.34
R_{merge} (last shell)	0.066 (0.53)	0.038 (0.54)	0.080 (0.39)
completeness (%) (last shell)	99.1 (97.2)	96.4 (95.6)	97.1 (89.6)
$\langle I/\sigma(I)\rangle$ (last shell)	16.6 (2.0)	24.1 (2.0)	10.5 (2.0)
χ^2 (last shell)	1.07 (1.06)	1.06 (1.19)	1.03 (1.00)

Table 2: Statistics of Structures of BLGA in Lattice Z

	pH 6.2	pH 7.1	pH 8.2
resolution limit (Å)	15.0−2.56	15.0−2.24	15.0−2.49
R_{free} (no. of reflections)	0.240 (545)	0.279 (557)	0.277 (576)
R (no. of reflections)	0.192 (5877)	0.233 (8736)	0.232 (6627)
no. of protein atoms	1286	1286	1286
no. of water molecules	115	62	101
RMS (bond distances) (Å)	0.009	0.008	0.005
RMS (bond angles) (deg)	1.6	1.5	1.4
Ramachandran plot[a] (%)			
core	82.6	83.9	81.2
allowed	15.4	14.8	18.1
generously allowed	1.3	0.7	0.0
disallowed	0.7	0.7	0.7
average *B* factor (Å^2)			
main chain	37.1	47.9	47.2
side chain	40.4	51.3	52.4
waters	67.4	70.9	69.3
accessible surface area (Å^2)			
monomer	8235	8458	8666
dimer	15524	15948	16165
lock and key[b]	15377	15865	16128

[a] As determined by PROCHECK (*44*). [b] For one pair of the chain of molecules formed by insertion of Lys8 of one molecule into a cavity of another molecule.

RESULTS AND DISCUSSION

Molecular Structure of Bovine BLGA in Lattice Z. The model for BLGA in lattice Z at pH 7.1, which has been refined to a resolution at 2.24 Å, will be used as the reference structure in the following discussion. BLGA in lattice Z folds into a calyx (see Figure 1), a motif typical of the lipocalin superfamily (*4*). The secondary structure is substantially that observed for BLG in lattice X (*29*), where eight antiparallel β strands, labeled β-A to β-H, fold with an up−

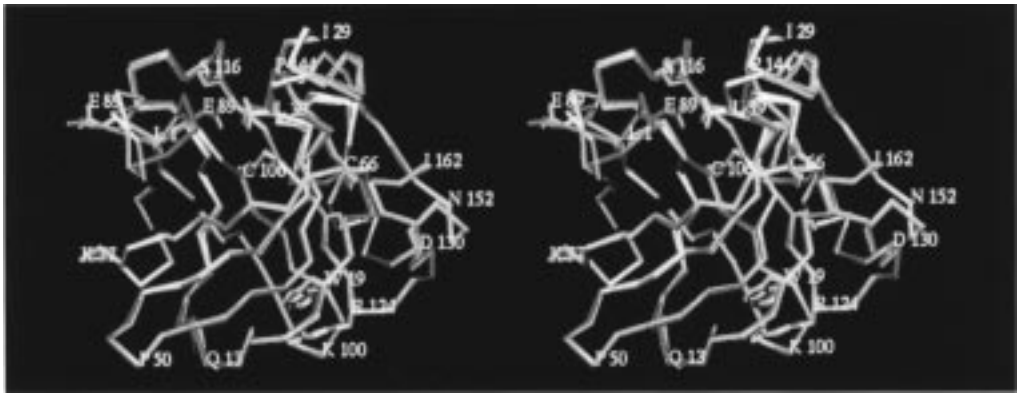

FIGURE 1: Stereo diagram of the Cα atom traces of BLGA structures in lattice Z at pH 6.2 (red), pH 7.1 (yellow), and pH 8.2 (blue). The side chains of Glu89 and the disulfide bridges connecting residues 106−119 and 66−160 are shown. Figure prepared with TURBO (*43*).

down−up−down topology to form the calyx. Attached to the calyx is a three-turn α helix, α-H, residues 129−142, which is followed by an extra β strand, β-I, through which BLG associates into dimers, forming an extended β sheet. Most of the hydrogen-bonding capacity of the β sheet is utilized, except for the long strand β-D (residues 64−77), across which the short strand β-E (residues 80−84) crosses approximately at right angles (see Figure 1). At the N terminus, a piece of extended strand, labeled β-0 (residues 4−8), makes a single hydrogen bond to strand β-F of the calyx. As is apparent in Figure 1, the only major difference in conformation as a function of pH occurs for loop EF (residues 85−90). At pH 6.2 loop EF is folded over the entrance to the calyx (closed conformation), as previously observed for lattice X (*29*) at a similar pH of 6.5. However, at pH 7.1 and 8.2, loop EF is folded back (open conformation) to reveal the interior of the calyx. This change and its functional implications are discussed later.

In addition to the helix α-H, the three short helices identified in the lattice X structure of BLG (*29*) are also found in this BLGA structure. These helices are labeled α-1, α-2, and α-3 and comprise residues 28−33 (in loop AB), 112−117 (in loop GH), and 152−158, respectively. Helix α-1 is a standard α helix in lattice Z, whereas it is a 3_{10} moiety in lattice X (*29*), and helices α-2 and α-3 are several residues longer in the lattice Z structure at pH 6.2 and 7.1. The α-H and α-3 helices are ended by 3_{10} turns; similarly to lattice X (*29*), residues 11−15 also form a short 3_{10} helix. With some exceptions, notably the 3_{10} helix spanning residues 11−15, these smaller secondary structural elements are not well conserved in the lipocalin family (*29*, *45*, *46*). Because the loop CD is connected to the C terminus via the disulfide bond Cys160−Cys66, α-3 may serve as a spring to restrain the flexible loop CD (average *B* factor of residues 61−67, 81 Å^2).

The average *B* factor of loop CD (residues 61−67) is very high, almost 70% higher than the overall average *B* factor. These residues appear at relatively low density in $2F_o - F_c$ maps (0.8−1.0 of the RMS value of the density), although the omit maps clearly show their existence, as illustrated in Figure 2A. The N terminus, residues 1−4, which is not included in the structure of BLG in lattice X (*29*), is well-defined in lattice Z, as illustrated in Figure 2B. The N-terminal α-amino group of Leu1 forms a salt bridge to Glu108, burying the latter side chain, as detailed in Table 3,

Table 3: Accessibility (in Å^2) of Titratable Residues and of Cys, Trp, and Tyr of BLGA at Different pH Values[a]

residue	pH 6.2	pH 7.1	pH 8.2	residue	pH 6.2	pH 7.1	pH 8.2
Leu1	181	186	144	Glu44	57	68	66
Arg40	24	23	21	Glu45	63	68	59
Arg124	47	53	49	Glu51	140	134	155
Arg148	100	100	94	Glu55	52	51	53
Lys8	203	190	187	Glu62	87	98	91
Lys14	115	110	118	**Glu65**	**132**	**103**	**140**
Lys47	73	74	88	Glu74	74	74	89
Lys60	19	39	32	**Glu89**	**4**	**116**	**136**
Lys69	75	92	87	Glu108	9	4	5
Lys70	119	120	114	Glu112	72	75	91
Lys75	123	123	128	**Glu114**	**87**	**126**	**124**
Lys77	202	206	211	Glu127	108	115	118
Lys83	113	96	92	**Glu131**	**107**	**68**	**105**
Lys91	**71**	**63**	**37**	Glu134	103	97	106
Lys100	133	138	142	Glu157	118	114	108
Lys101	71	70	73	Glu158	80	83	88
Lys135	74	64	85	His146	130	126	127
Lys138	104	116	138	His161	10	12	13
Lys141	167	160	167	Cys66	34	36	38
Asp11	69	65	66	Cys160	0	0	9
Asp28	57	63	64	Cys106	1	1	1
Asp33	85	95	99	Cys119	1	1	1
Asp53	27	34	33	Cys121	0	0	0
Asp64	129	133	123	Trp19	5	2	3
Asp85	**152**	**131**	**72**	Trp61	60	59	59
Asp96	31	34	36	Tyr20	44	40	51
Asp98	44	35	40	Tyr42	0	0	3
Asp129	26	41	33	Tyr99	37	30	38
Asp130	115	105	110	Tyr102	17	10	14
Asp137	66	64	63	Ile162	121	130	110

[a] Analyzed by programs AREAIMOL and RESAREA of the CCP4 suite (*47*). Residues for which the accessible area changes by more than 30 Å^2 are highlighted in bold.

which summarizes solvent accessibilities of various residues with charged side chains.

In some crystal forms the C terminus of BLG is poorly ordered, and the disulfide bond linking Cys160 to Cys66 is difficult to observe. In contrast, the disulfide bonds of BLGA in lattice Z are both clearly defined, not only that linking Cys119 to Cys106 but also that linking Cys160 to Cys66, as illustrated in Figure 2A. The configurations and the accessibilities of these two disulfide bonds are different. The distance between Cα106 and Cα119 is only 3.83 Å, while the distance between Cα160 and Cα66 is 5.91 Å. The former disulfide bond appears much more rigid. The solvent-accessible area of the disulfide bond at Cys160−Cys66 is 36 Å^2 and coincides with a higher than average *B* factor for this region [for atoms within 6 Å of Cys66 and Cys160,

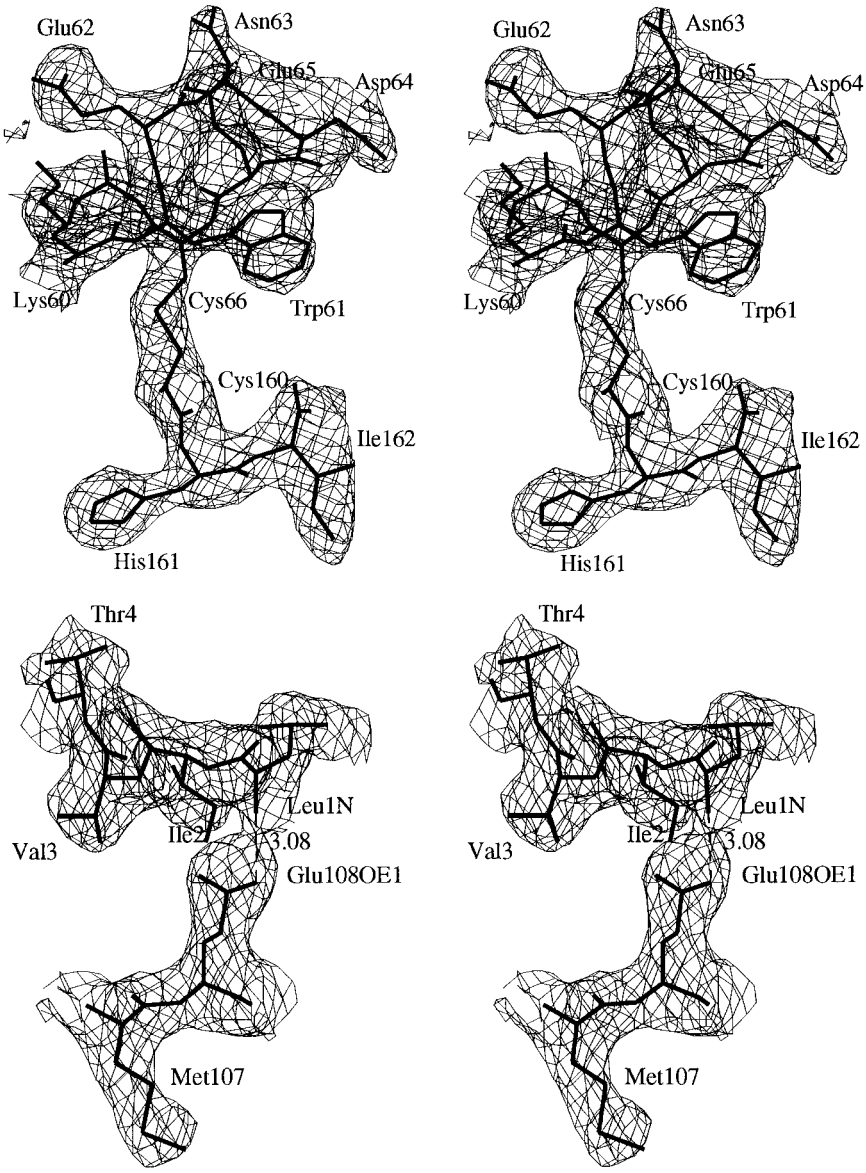

FIGURE 2: Electron density maps of selected regions of BLGA in lattice Z. Figure prepared with TURBO (*43*). (A, top) Stereo diagram of loop CD at pH 7.1, residues 60−67 and 160. The final model is superimposed on a $2F_o - F_c$ omit map (calculated with residues 61−65 omitted), contoured at 1.0σ. (B, bottom) Stereo diagram of the N terminus of BLGA at pH 7.1, residues 1−4 and 108. The final model is superimposed on a $2F_o - F_c$ omit map (calculated with residues 1−4 omitted), contoured at 1.0σ.

B(average) = 58 Å^2], while the other disulfide bond has an accessible surface area of only 1.0 Å^2 and is located in a well-ordered region with lower than average *B* factors [for atoms within 6 Å of Cys106 and Cys119, *B*(average) = 31 Å^2]. Both disulfide bonds have typical C−S−S−C torsion angles of ~100°.

Intermolecular Interactions of BLGA in Lattice Z. The space group of lattice Z is $P3_221$. There are six asymmetric units, each containing one monomer, per unit cell. There are four regions involved in three distinct intermolecular contacts of BLGA. The first interface, the dimer interface, has been previously described and illustrated in detail for the structure of BLG in lattice X (*29*). This dimer interface is also found in lattice Y (*30*)[2] and presumably persists in solution; it is comprised of antiparallel strands β-I and residues 29−35 of loop AB. In lattice Z (but not X), the monomer units are related by a 2-fold crystallographic axis. At pH 7.1 and 8.2 ordered water molecules are found in the channel that is formed by the pair of α-H helices, which lie above the β-I strands. The dimer interface buries ~970 Å^2 of the accessible area per dimer at pH 7.1 (~950 Å^2 at pH 6.2, ~1010 Å^2 at pH 8.2) (*47*). These numbers are similar to those calculated for BLG in lattice X (~1140 Å^2 at pH 6.5) (*29*). The percentage of the surface area buried per monomer of BLGA in lattice Z remains constant, however, at 5.74%, 5.75%, and 5.84% at pH 6.2, 7.1, and 8.2, respectively. These percentages lie at the lower end of the range typically found for strongly associated dimers (*48*). There are, however, small but significant differences in the orientation of the second molecule of the dimer with a change in pH for BLGA in lattice Z and a rather larger difference in orientation between lattice Z and lattice X, as illustrated in Figure 3.

The second interface, which is illustrated in Figure 4 and does not appear to have been described previously, involves the side chain of Lys8 from one molecule acting as a "key", which inserts into a "lock" provided by a neighboring molecule. The lock is formed by Tyr20 and Ser21 from the

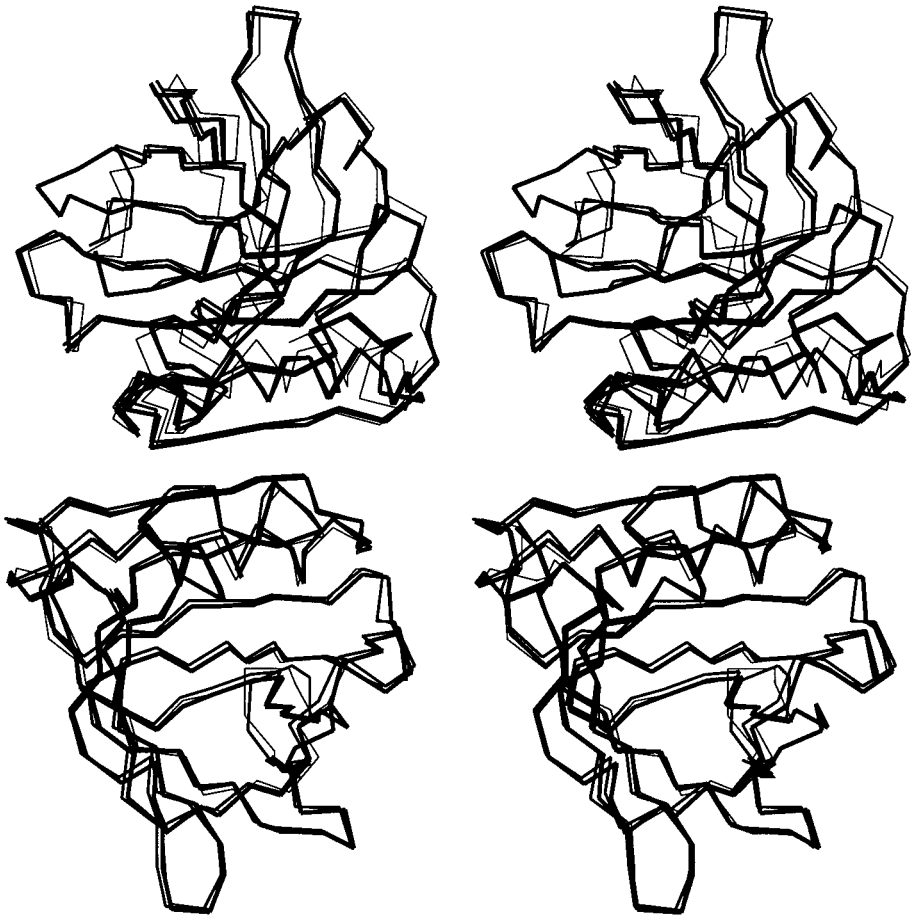

FIGURE 3: Differences in the dimer interface between BLG in lattice X (thin lines) and BLGA in lattice Z at pH 6.2 and 7.1 (increasingly thicker lines). To highlight differences, the superposition is optimized for one molecule of the dimer. Figure prepared with TURBO (*43*).

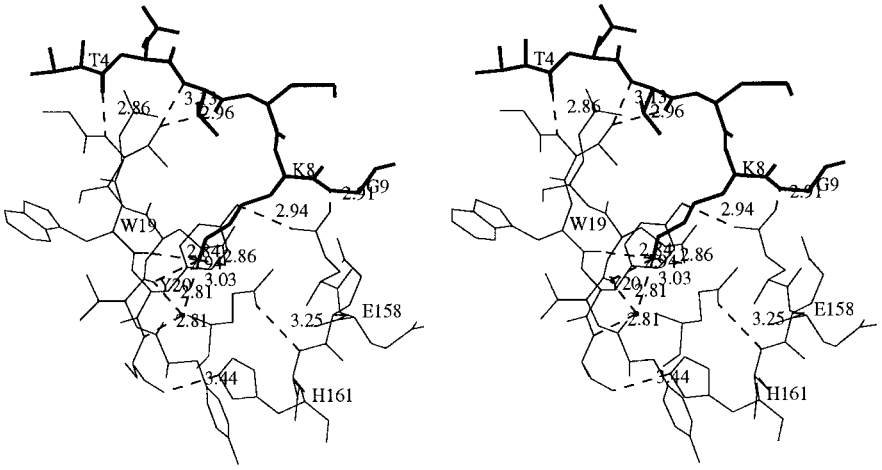

FIGURE 4: Stereo diagram of the "lock and key" interface of BLGA. Lys8 and surrounding residues from one molecule (the key) are drawn with thick lines. The residues forming the "lock" are drawn with thin lines. Hydrogen bonds are shown as dotted lines. Figure prepared with TURBO (*43*).

end of the first half of the β-A strand; Val41, Tyr42, Val43, and Glu44 from the middle of the β-B strand; and Leu156, Glu157, and Glu158 from the α-3 helix, together with the side chain of His161. The bottom of this hole contains a water molecule, which bridges the peptide moieties of Val43 and Ser21 via hydrogen bonds. This water molecule is also hydrogen bonded to the inserted Lys8's ammonium group. The insertion of Lys8 leads to formation of several hydrogen bonds, detailed in Table 4. In addition to these hydrogen bonds, there are extensive van der Waals contacts in this interface. A total of 1050 Å^2 of accessible area (*47*) is buried at pH 7.1 (1090 Å^2 at pH 6.2, 990 Å^2 at pH 8.2). This "lock and key" interface is, therefore, quite substantial and leads to a linear chain array of BLGA molecules in lattice Z. These interactions may be involved in the gelling properties of BLG (*49*, *50*). The percentage of surface area buried in this interface per dimer decreases with increasing pH: 6.64% at pH 6.2, 6.18% at pH 7.1, and 5.69% at pH 8.2. This intermolecular interaction does not occur in either lattice X (*29*) or lattice Y (*30*).

Table 4: Hydrogen Bonds of the Lock and Key Interface of BLGA

key residue	atom	distance (Å)	lock atom	residue
Lys8	NZ	2.9	OE2	Glu44
Lys8	NZ	2.9	O	Val43
Lys8	NZ	2.8	O	Trp19
Lys8	NZ 3.0	water[a] 2.8	N	Ser21
Lys8	NZ 3.0	water[a] 2.8	O	Val43
Thr4	O	2.9	N	Thr18
Thr6	N	3.1	OG1	Thr1
Thr6	O	3.0	OG1	Thr18
Gly9	N	2.9	OE1	Glu157

[a] A buried water is hydrogen bonded between NZ of Lys8 and the main-chain N of Ser21 and O of Val43.

The final interface is the loop interface which is formed from loops CD, EF, and GH. Space group $P3_221$ has two 2-fold crystallographic symmetry axes. One of them passes through the dimer interface described above, while the other 2-fold axis places pairs of the loops CD, EF, and GH into mutual contact. There do not appear to be any specific interactions among these rather mobile regions, whose proximity caused some difficulty in the interpretation of electron density maps. These loops, especially loop EF (residues 85−90), form the doorway to the interior of the BLGA calyx.

BLGA molecules in lattice Z are packed layer by layer, perpendicular to the *c*-axis of the crystal. Each layer is rotated by 60° with respect to an adjacent layer. Within one layer, BLGA molecules form parallel chains via the lock and key interfaces. The loop interfaces act as a cushion between adjacent chains. The dimer interfaces of one chain are interleaved and face up and down along the crystallographic *c*-axis. In another simple point of view, BLGA molecules are packed as parallel dimer chains. A general loosening of intermolecular contacts in the lock and key interface is observed as the pH increases.

Potential Ligand-Binding Sites of BLGA. By analogy with retinol-binding protein (*28*, *45*, *46*) and other proteins of the lipocalin superfamily, the inside of the β-lactoglobulin calyx appears to be the major ligand binding site (*23*). The surface of the interior of the calyx, which involves exclusively hydrophobic side chains from residues[3] **Leu10**, Ile12, Val15, Val41, Val43, Leu46, **Leu54**, Ile56, **Leu58**, Ile71, Ala73, Ala80, **Phe82**, Ile84, Val92, Val94, Leu103, Phe105, and Met107, appears to complement well the surface of retinol, as illustrated in Figure 5A (*51*) for BLGA at pH 7.1 (open conformation of loop EF) and as proposed previously (*23*, *29*, *52*). This complementarity is also present at pH 6.2 and 8.2, except that at pH 6.2 the retinol would be totally buried underneath loop EF, which is in the closed conformation (Figure 5B,C); in this case the OE1 atom of **Glu89**[3] could form a hydrogen bond with the retinol OH group, while the OE2 atom of **Glu89** is adjacent to the peptide O atom of Ser116. Assigning the carboxyl residue with the anomalous pK_a of 7.3 to Glu89, then at pH 6.2 the carboxyl oxygen OE2 should be protonated and, therefore, hydrogen bonded to Ser116O. The side chains of residues Leu46 and Leu103 lie between the side chain of **Trp19**[3] and the β-ionone ring of retinol in our model. This model differs in detail from

[3] Residues that are invariant across 17 different β-lactoglobulins are highlighted in boldface type.

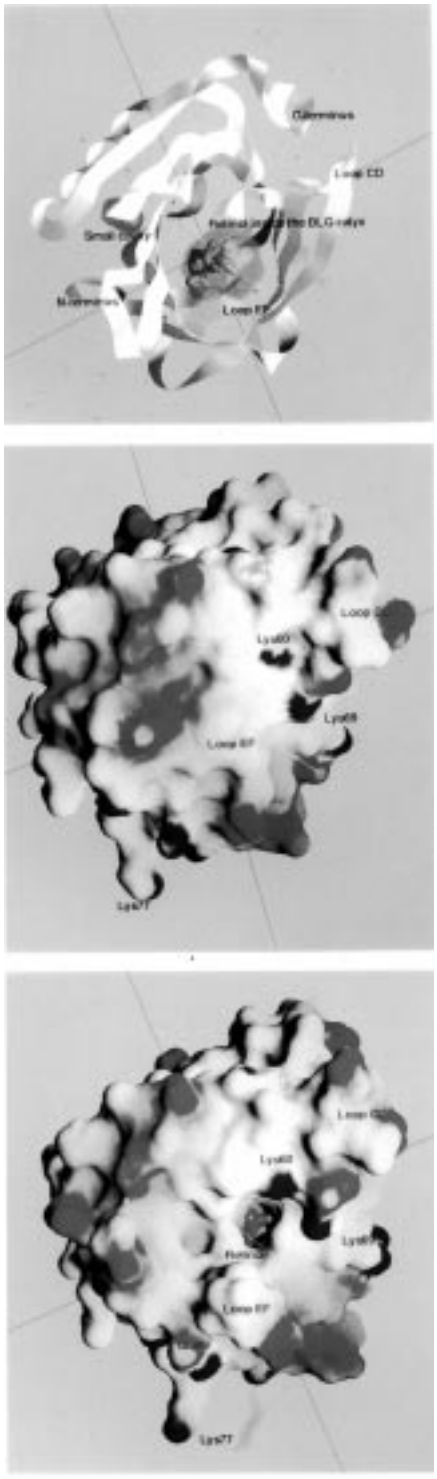

FIGURE 5: Molecular surface of BLGA in lattice Z. All the surfaces have been rendered with program GRASP (*51*). External surfaces are colored blue for positively charged regions of the surface and red for negatively charged regions. (A, top) Ribbon-type diagram of the main chain of BLGA in lattice Z at pH 6.2. A retinol molecule (orange) has been fit into the calyx cavity (green). The side chain of Cys121 points into a small cavity (blue), which lies between the three-turn α helix and the outside of the cavity. (B, middle) Molecular surface at pH 6.2; same orientation as in (A). Loop EF covers the entrance to the calyx cavity. (C, bottom) Molecular surface at pH 7.1, with the molecule in the same orientation as in (A) and (B). Loop EF flips to expose the interior of the calyx. A retinol molecule (red) lies at the base of the deep hole. The molecular surface at pH 8.2 is very similar.

other models for the BLG−retinol complex. An early model for retinol binding to BLG placed the retinol deeper inside the calyx (*23*) and directed away from loop EF, compared to that proposed here. A later model for retinol and retinoic acid binding (*52*) proposed interaction of the headgroup with Lys70 [Lys69 in the revised structure (*29*, *30*)] and proximity of the β-ionone ring to **Trp19** on the basis of fluorescence quenching (*52*). In both of these models, the position and orientation of the retinol ligand are different from that observed crystallographically for the human (*45*) and bovine (*46*) RBP−retinoid complexes, in that the retinol is buried more deeply inside the calyx of BLG and its long axis is tilted (*23*, *52*). In our model (Figure 5A) the retinol is also located deeper inside the BLG calyx, but compared to the RBP−retinol complexes, the retinol is similarly oriented, except for a rotation of approximately 180° about its long axis. At pH 6.2, a trail of electron density is clearly visible inside the calyx, immediately under the lid, loop 85−90. Modeled as water molecules, satisfactory refinement (including lowering of R_{free}) is obtained ($B \sim 50$ Å^2, $H_2O\cdots H_2O$ 2.7−3.0 Å). However, no hydrogen-bonding contact with the main protein chain is observed, and contacts with the hydrophobic side chains are greater than 3.6 Å. While no potential ligand was included in the protein purification, we cannot eliminate the possibility that this density is part of a hydrocarbon chain. At pH 7.1 and 8.2, no ordered electron density inside the calyx is observed.

Besides the traditional binding site discussed above, another potential binding site for small molecules appears to exist. In lattice Z, strands β-F, β-G, and β-H, the second half of β-A, and β-I create a flat β sheet, as shown in Figures 1, 3, and 5A. This β sheet is mostly covered by the N terminus and α-H, thereby creating a small cavity immediately adjacent to SG Cys121, to which a methylmercuric ion can bind with negligible rearrangement of main-chain and side-chain groups (*30*).[2] However, introducing a bulky moiety to this small cavity may disturb the secondary structure, such as helix α-H and strand β-A, which surrounds this site. The disturbance may be transferred to the β-I strand through the β sheet and indirectly influence the dimer interface of β-lactoglobulin. Thus, modified BLG may have different association behavior compared to native BLG. Ralston (*53*) showed that BLG, which was chemically modified by blocking a sulfhydryl group with *N*-ethylmaleimide, exhibited different characteristics for pH-dependent phenomena.

Behavior of BLGA during the Tanford Transition. To date, no substantiated structural basis has been found for the various pH-dependent phenomena of BLG, in particular for the location of the carboxylic acid/carboxylate group implicated by Tanford et al. (*35*) in titration studies and tentatively assigned as Glu89 by Brownlow et al. (*29*). The structures of BLGA at different pH values provide a pseudodynamic view of BLGA during the pH-induced transition, unencumbered by comparisons across crystal forms and by sample heterogeneity.

The earliest observed pH-dependent property of BLG was that an increase in pH (from 6 to 8) was accompanied by a decrease in sedimentation coefficients (*32*), which can now be attributed to an overall increase in molecular volume/surface area: the accessible surface area of BLGA increases from 8240 Å^2 at pH 6.2 to 8460 Å^2 at pH 7.1 to 8670 Å^2 at pH 8.2, as summarized in Table 2. In terms of dimers, the probable association state of BLG in solution over this pH range and at room temperature, the accessible surface area increases from ∼15 520 Å^2 at pH 6.2 to ∼15 950 Å^2 at pH 7.1 to ∼16 320 Å^2 at pH 8.2. This is a factor responsible for the swelling of the unit cell of BLGA in lattice Z. The increase in accessible surface area is associated with a small *increase* of ∼6% in buried surface at the dimer interface, from 950 Å^2 at pH 6.2 to 1010 Å^2 at pH 8.2, an increase that appears incompatible with electrophoretic evidence that at high pH BLG dimers dissociate more readily (*54*). However, as structural results essentially show only the enthalpic contribution to the free energy for the dimer ⇔ monomer equilibrium, the small increase in buried surface area (or the absence of a decrease) with increase in pH, while surprising, is not incompatible with thermodynamic data, as entropic effects are not necessarily apparent in the structure.

Table 5: Displacements (in Å) for Cα Atoms of BLGA at pH 6.2, 7.1, and 8.2[a]

	pH 6.2	pH 7.1	pH 8.2	X (pH 6.5)
pH 6.2		0.24	0.26	0.45
pH 7.1	0.95		0.24	0.50
pH 8.2	0.98	0.38		0.51
X (pH 6.5)	0.61	1.16	1.16	

[a] Calculated by means of LSQKAB (*47*). The entries above the diagonal are for the calyx core of nine β strands and the three-turn α helix characteristic of lipocalins [calyx core: strands β-A(15−27), β-B(40−50), β-C(52−62), β-D(64−77), β-E(80−84), β-F(90−98), β-G(101−110), β-H(117−125), and β-I(146−152) and α helix (128−142)]. The entries below the diagonal are for the entire molecule. BLG in lattice X (*29*) is included for comparison.

Except for loop EF (residues 85−90), the BLGA calyx experiences only minor changes in conformation as a function of pH, as shown in Figures 1, 3, and 5B,C. Pairwise superpositions, calculated via TURBO (*43*), of the three BLGA structures (lattice Z, pH 6.2, 7.1, and 8.2) lead to RMS differences of less than 0.21 Å for the Cα atoms of 144 residues out of 162 that satisfy the criterion of a maximum displacement in Cα atoms of 0.5 Å. RMS displacements for the whole molecule and for just the calyx core, calculated by LSQKAB (*47*), are summarized in Table 5. The RMS displacements between the lattice X and lattice Z structures, for the core calyx, are somewhat larger at ∼0.5 Å, indicating a small degree of conformational variability in the core calyx.

The omit electron density maps for loop EF, in its two conformations, are shown in panels A and B of Figure 6, and the superposition of BLGA in the vicinity of loop EF at pH 6.2 and 7.1 is shown in Figure 6C. At low pH, loop EF serves as a door or lid to block access to the calyx. At high pH, loop EF flips away from the calyx, which then becomes accessible for ligands. In addition, this conformational change leads to Glu89 changing from a buried situation at low pH to exposed at high pH; see Figures 1 and 5. The solvent-accessible area of Glu89 is 4 Å^2 at pH 6.2, 116 Å^2 at pH 7.1, and 136 Å^2 at pH 8.2, as detailed in Table 3. Indeed, the 4 Å^2 accessible surface area of Glu89 at pH 6.2 is contributed by its carbonyl oxygen atom, and the COOH group of Glu89 is totally buried. The side chain of Glu89 at low pH is mostly surrounded by hydrophobic residues, but the presumably protonated carboxyl atom OE2 forms a hydrogen bond with the carbonyl oxygen atom of Ser116

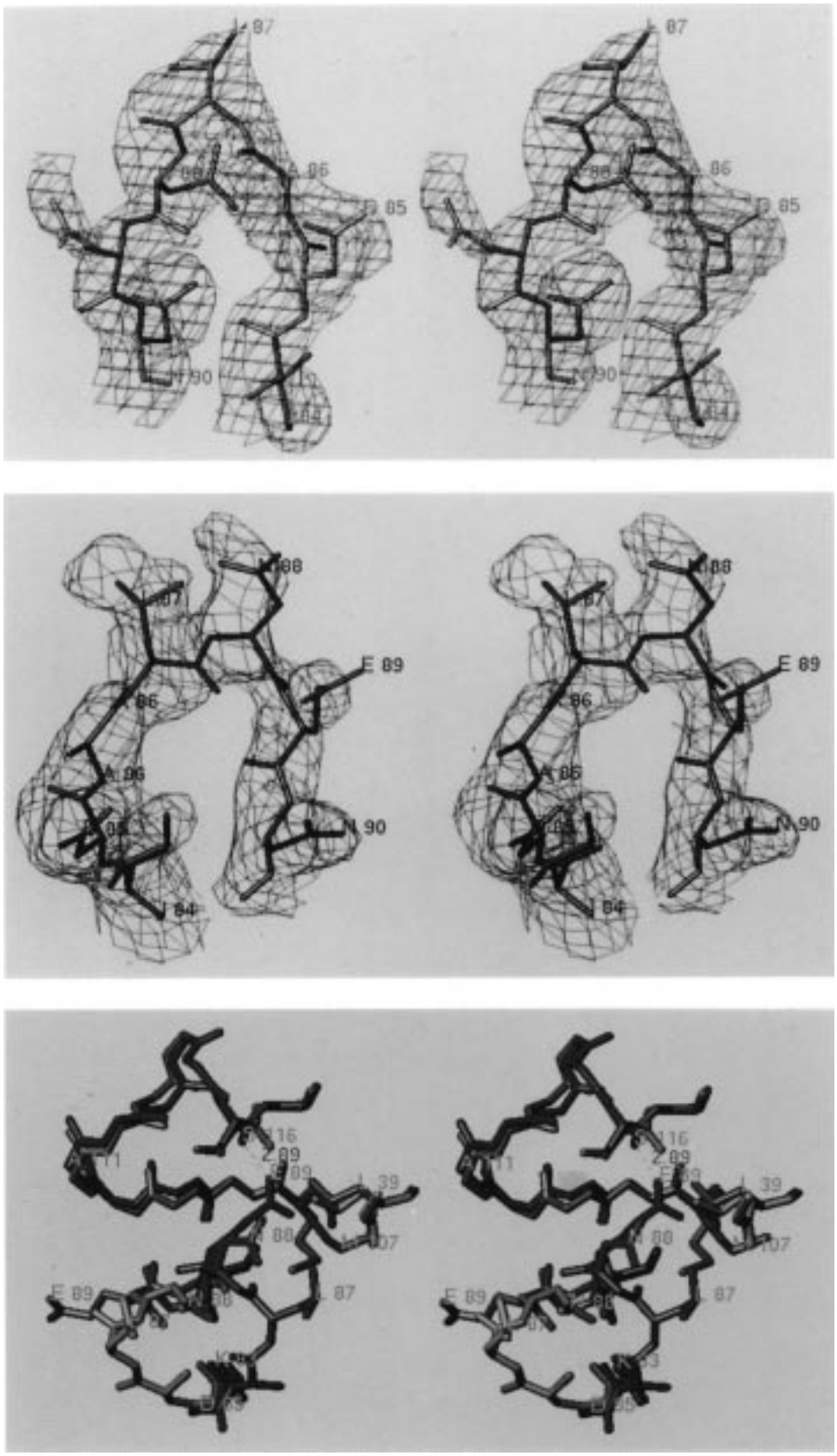

FIGURE 6: Stereo diagrams of electron density for loop EF of BLGA in lattice Z at pH 7.1 and 6.2. Figure prepared with TURBO (*43*). (A, top) pH 7.1 (open conformation of loop EF): Superposition of the final positions of residues 85−90 on a $2F_o - F_c$ omit map (residues 86−89 omitted), contoured at 0.5σ. (B, middle) pH 6.2 (closed conformation of loop EF): Superposition of the final positions of residues 85−90 on a $2F_o - F_c$ omit map (residues 86−89 omitted), contoured at 0.5σ. To avoid overlap, the orientation is not the same as that for (A). (C, bottom) Stereo diagram of loop EF for the superposition of BLGA in lattice Z at pH 6.2 (red, closed conformation) with that at pH 7.1 (yellow, open conformation).

(2.8 Å). Thus, at pH 6.2, the carboxyl group of Glu89 is unavailable for titration. When deprotonated at high pH, the buried charge of the carboxylate group of Glu89 triggers the expulsion of this group, with the associated movement

of loop EF in which Glu89 is situated. This is consistent with the titration behavior of BLG and with the anomalous carboxylate pK_a of ~7.3 found for BLG (*35*). The conformational changes in loop EF begin at residue 85, when approaching the loop from the N terminus, and at residue 90, when approaching the loop from the C terminus, as illustrated in Figure 6C. As detailed in Table 3, no other charged residue undergoes a change from buried to exposed as a function of pH, although the main chain of Asp85 becomes partially buried at pH 8.2. In the closed, low-pH conformation, the hydrophobic side chain of Leu87 is partly buried and in contact with hydrophobic side chains (or portions thereof) of residues Leu39 and Lys60. In the high-pH open conformation, these side chains become more exposed and in the case of Leu87 completely exposed. A previous observation that Glu89 is buried at pH 7.8 in lattice Z (*29*) appears to be in contradiction with our observations that at pH 7.1 and 8.2 this residue is exposed to solvent. However, the two structures are not strictly comparable, since (i) the material used in the cited study (*29*) is a mixture of variants A and B, (ii) the data in the cited structure (*29*) extend only to 3 Å resolution, and (iii) the Tanford transition is sensitive to ionic strength.

In addition to the anomalous carboxylate at residue 89, increased exposure for three of the four tyrosine residues with change in pH across the Tanford transition has been identified (*55*, *56*). We have been unable to identify a significant change in the environment of any tyrosine that is directly linked to the pH-induced conformational change in the EF loop, for either monomers (see Table 3) or dimers. The conformational change of loop EF is propagated into reorientations of the side chains for Met107, Ile84, and to a lesser extent Leu39. The environments of tyrosine residues at positions 20, 42, and 99 appear to remain unchanged at pH 6.2, 7.1, and 8.2. Tyr102, however, remains unmoved by changes in pH but it is in the vicinity of a chain of conformational changes involving the side chains of charged residues beginning with Lys135 and extending to Glu131 and Glu134. Whether these changes are intrinsic to BLG in solution, or are associated with changes in crystal packing, remains uncertain. Examination of intermolecular contacts as a function of pH reveals that no tyrosine is close to the dimer interface. Although Tyr20 of one molecule lies alongside Lys8 of another in the lock and key intermolecular interface, this interface is unlikely to be responsible for the observation of dimers in dilute solutions. Tyr20 and Tyr99 may be tentatively identified as the tyrosines most susceptible to chemical modification by *N*-acetylimidazole at pH 7.5 (*56*). Tyr20 is partly buried by the flexible fragment 156−158, whose conformation varies with lattice type (*29*, *30*), and for Tyr99 the edge of the aromatic ring and the hydroxyl group are exposed to solvent. Tyr42, which remains buried at the pH values of this study, can be identified as the tyrosine residue that remains buried and inaccessible to chemical modifiers, such as cyanuric acid (*57*) and *N*-acetylimidazole (*56*), and to titration until the pH is above 12 (*56*).

The reactivity increase of Cys121 at high pH is not directly related to the opening of the calyx lid at high pH. Although the opening permits access to the Cα atom of Cys121, the SH group points away from the interior of calyx and into the small cavity of BLGA; see Figure 5A. There are a number of hydrophobic residues in the immediate vicinity, and at the surface some charged residues, Lys101, Lys135, Arg148, Asp129, Asp137, Glu131, and Glu134, are within 8 Å of the SH group. At pH 6.2, these residues provide a less negatively charged environment, and the average *B* factor of atoms within 8 Å of the Cys121 SG atom is 16.2 Å^2. Increasing the pH to 7.1 will change the static charge to a more negatively charged state (favoring the access of positively charged reagents). In addition, the average *B* factor of atoms within 8 Å of the Cys121 SG atom increases to 30.0 Å^2. This implies that increasing the pH above 6.7 (*37*) will favor (thermodynamically) the binding of a positively charged reagent to the SG atom of Cys121 and increase (kinetically) the susceptibility of this thiol to chemical modification, even though the solvent accessibilities of Cys121 do not change with pH, at least in the 3-D structures of BLGA (see Table 3).

Functional Significance of the pH-Dependent Conformation of BLGA. The Tanford transition has been observed not only in bovine β-lactoglobulins but also in goat β-lactoglobulin (*58*). The key residue of the Tanford transition, Glu89, is one of only 21 conserved residues through all currently sequenced β-lactoglobulins (SwissProt, *59*), as aligned by CLUSTALW (*60*) and summarized in Table 6 (Supporting Information). This suggests that pH control of access to the interior of the calyx of BLGA may have functional implication. It is well-known that the pH environment of the digestive canal changes from acidic in the stomach to basic in the small intestine and that BLG remains intact on passage through the acidic proteolytic environment of the stomach (*21*). The pH-dependent conformation of fragment EF may be related to the physiological function of β-lactoglobulin in vivo: the closed calyx, characteristic of BLG at low pH, protects the ligand in the acidic stomach, while the opened calyx, characteristic of BLG at high pH, permits release of the ligand in the small intestine for absorption.

CONCLUSIONS

BLGA undergoes significant conformational changes as the pH changes from 6.2 to 8.2, as inferred from a variety of chemical and physical evidence. The structures of BLGA in lattice Z at pH 6.2, 7.1, and 8.2 provide insight into these changes. As the pH is increased, there is an expansion in the volume of BLGA. In addition to the previously well-characterized dimer interface, there is in lattice Z a substantial interface created by insertion of Lys8 into a pocket of a neighboring molecule. Loop EF (residues 85−90) forms a lid to the calyx, which is closed at pH 6.2 and open at pH 7.1 and 8.2. Glu89, which is buried at pH 6.2, becomes exposed at pH 7.1 and 8.2. This conformational change accounts for the physical and chemical pH-dependent properties of BLG and has functional implications for the reversible binding and release of ligands.

ACKNOWLEDGMENT

We acknowledge helpful discussions with Gavin Manderson, Phillip A. Jeffrey, Gillian E. Norris, and Lindsay Sawyer.

SUPPORTING INFORMATION AVAILABLE

Table 6 showing the sequence alignment of β-lactoglobulins (2 pages). Ordering information is given on any current masthead page.

REFERENCES

1. Bell, K., and McKenzie, H. A. (1964) *Nature 204*, 1275−1279.
2. Palmer, A. H. (1934) *J. Biol. Chem. 104*, 359−372.
3. Crowfoot, D. M., and Riley, D. P. (1938) *Nature 141*, 521−522.
4. Flower, D. R., North, A. C. T., and Attwood, T. K. (1993) *Protein Sci. 2*, 753−761.
5. O'Neill, T. E., and Kinsella, J. E. (1987) *J. Agric. Food Chem. 35*, 770−774.
6. Farrell, H. M., Bede, M. J., and Enyeart, J. A. (1987) *J. Dairy Sci. 70*, 252−258.
7. Robillard, K. A., and Wishnia, A. (1972) *Biochemistry 11*, 3835−3840, 3841−3845.
8. Dufour, E., and Haertle, X. (1990) *Protein Eng. 4*, 185−190.
9. Liberatori, J., Guidetti, L. M., and Conti, A. (1979) *Boll. Soc. Ital. Biol. Sper. 55*, 815−821.
10. Liberatori, J., Morisio, L., Guidetti, L. M., Conti, A., and Napolitano, L. (1979) *Boll. Soc. Ital. Biol. Sper. 55*, 1369−1373.
11. Halliday, J. A., Bell, K., and Shaw, D. C. (1991) *Biochim. Biophys. Acta 1077*, 25−30.
12. Lyster, R. L. J., Jenness, R., Phillips, N. I., and Sloan, R. E. (1966) *Comp. Biochem. Physiol. 17*, 967−971.
13. Hambling, S. G., McAlpine, A. S., and Sawyer, L. (1992) in *Advanced Dairy Chemistry: 1. Proteins* (Fox, P. F., Ed.) pp 141−190, Elsevier Applied Sciences, New York.
14. Eigel, W. N., Butler, J. E., Ernstrom, C. A., Farrell, H. M., Jr., Harwalkar, V. R., Jenness, R., and Whitney, R. M. (1984) *J. Dairy Sci. 67*, 1599−1631.
15. Conti, A., Napolitano, L., Cantisani, A. M., Davoli, R., and Dall'Olio, S. (1988) *J. Biochem. Biophys. Methods 16*, 205−214.
16. Godovac-Zimmermann, J., Krause, I., Baranyi, M., Fischer-Frühholz, S., Juszczak, J., Erhardt, G., Buchberger, J., and Klostermeyer, H. (1996) *J. Protein Chem. 15*, 743−750.
17. Godovac-Zimmermann, J., Conti, A., Sheil, M., and Napolitano, L. (1990) *Biol. Chem. Hoppe-Seyler 371*, 871−879.
18. Hill, J. P., Boland, M. J., Creamer, L. K., Anema, S. G., Otter, D. E., Paterson, G. R., Lowe, R., Motion, R. L., and Thresher, W. C. (1996) in *Macromolecular Interactions in Food Technology*, Chapter 22, pp 281−294, American Chemical Society, Washington, DC.
19. Kella, N. K. D., and Kinsella, J. E. (1988) *Biochem. J. 255*, 113−118.
20. Reddy, I. M., Kella, N. K. D., and Kinsella, J. E. (1988) *J. Agric. Food Chem. 36*, 737−741.
21. Yvon, M., Van Hille, I., Péllisier, J.-P., Guilloteau, P., and Toullec, R. (1984) *Reprod. Nutr. Dev. 24*, 835−843.
22. Pérez, M. D., Sanchez, L., Aranda, P. P., Ena, J. M., and Calvo, M. (1990) *Cell. Mol. Biol. 36*, 205−231.
23. Papiz, M. Z., Sawyer, L., Eliopoulos, E. E., North, A. C. T., Findley, J. B. C., Sivaprasadarao, R., Jones, T. A., Newcomer, M. E., and Kraulis, P. J. (1986) *Nature 324*, 383−385.
24. Pérez, M. D., and Calvo, M. (1995) *J. Dairy Sci. 78*, 978−988.
25. Liberatori, J., Guetti, L. M., and Conti, A. (1979) *Boll. Soc. Ital. Biol. Sper. 55*, 822−825.
26. Aschaffenburg, R., Green, D. W., and Simmons, R. M. (1965) *J. Mol. Biol. 13*, 194−201.
27. Green, D. W., Aschaffenburg, R., Camerman, A., Coppola, J. C., Diamand, R. D., Dunnill, P., Simmons, R. M., Komorowski, E. S., Sawyer, L., Turner, E. M. C., and Woods, K. F. (1979) *J. Mol. Biol. 131*, 375−397.
28. Newcomer, M. E., Jones, T. A., Åqvist, J., Sundelin, J., Eriksson, U., Rask, L., and Peterson, P. A. (1984) *EMBO J. 3*, 1451−1454.
29. Brownlow, S., Cabral, J. H. M., Cooper, R., Flower, D. R., Yewdall, S. J., Polikarpov, I., North, A. C. T., and Sawyer, L. (1997) *Structure 5*, 481−495.
30. Bewley, M. C., Qin, B. Y., Jameson, G. B., Sawyer, L., and Baker, E. N. (1997) Bovine β-lactoglobulin and its variants: a three-dimensional perspective, in *Milk Protein Polymorphism*, pp 100−109, International Dairy Federation Bulletin Special Issue 9702, IDF, Brussels.
31. Monaco, H. L., Zanotti, G., Spadon, P., Bolognesi, M., Sawyer, L., and Eliopoulos, E. E. (1987) *J. Mol. Biol. 197*, 695−706.
32. Pedersen, K. O. (1936) *Biochem. J. 30*, 961−970.
33. Groves, M. L., Hipp, N. J., and McMeekin, T. L. (1951) *J. Am. Chem. Soc. 73*, 2790−2793.
34. McKenzie, H. A., and Sawyer, W. H. (1967) *Nature 214*, 1101−1104.
35. Tanford, C., Bunville, L. G., and Nozaki, Y. (1959) *J. Am. Chem. Soc. 81*, 4032−4035.
36. Qi, X. L., Brownlow, S., Holt C., and Sellers, P. (1995) *Biochim. Biophys. Acta 1248*, 43−49.
37. Dunnill, P., and Green, D. W. (1965) *J. Mol. Biol. 15*, 147−151.
38. Otwinowski, Z. (1996−1997) Data processing system, Version 1.9.1, University of Virginia Patent Foundation.
39. Otwinowski, Z. (1996−1997) Data processing system, Version 1.9.0, University of Virginia Patent Foundation.
40. Navaza, J. (1994) *Acta Crystallogr. A50*, 157−163.
41. Brünger, A. T. (1988−1992) X-PLOR Manual, Version 3.1f, Yale University, New Haven, CT.
42. Brünger, A. T. (1992) *Nature 355*, 472−475.
43. Cambillau, C., Roussel, A., Inisan, A. G., and Knoops-Mouthuy, E. (1996) TURBO−FRODO version 5.5, BioGraphics, AFMB-CNRS, Marseille, France.
44. Laskowski, R. A., MacArthur, M. W., Moss, D. S., and Thornton, J. M. (1993) *J. Appl. Crystallogr. 26*, 283−291.
45. Cowan, S. W., Newcomer, M. E., and Jones, T. A. (1990) *Proteins: Struct., Funct., Genet. 8*, 44−61.
46. Zanotti, G., Berni, R., and Monaco, H. L. (1993) *J. Biol. Chem. 268*, 10728−10738.
47. Collaborative Computing Project No. 4 (1994) The CCP4 suite of programs for protein crystallography, *Acta Crystallogr. D50*, 760−763.
48. Jones, S., and Thornton, J. M. (1995) *Prog. Biophys. Mol. Biol. 63*, 31−65.
49. Huang, X. L., Catignani, G. L., Foegeding, E. A., and Swaisgood, H. E. (1994) *J. Agric. Food Chem. 42*, 1064−1067.
50. McSwiney, M., Singh, H., Campanella, O., and Creamer, L. K. (1994) *J. Dairy Res. 61*, 221−232.
51. Nicholls, A., Sharp, K., and Honig, B. (1991) *Proteins: Struct., Funct., Genet. 11*, 281−296.
52. Cho, Y. J., Batt, C. A., and Sawyer, L. (1994) *J. Biol. Chem. 269*, 11102−11107.
53. Ralston, G. B. (1972) *C. R. Trav. Lab. Carlsberg 38*, 499−512.
54. Georges, C., and Guinand, S. (1960) *J. Chem. Phys. 57*, 606−614.
55. Pantaloni, D. (1965) Doctoral Dissertation, University of Paris, France.
56. Townend, R. J., Herskovits, T. T., Timasheff, S. N., and Gorbunoff, M. J. (1969) *Arch. Biochem. Biophys. 129*, 567−580.
57. Gorbunoff, M. J. (1967) *Biochemistry 6*, 1606−1615.
58. Ghose, A. C., Chaudhuri, S., and Sen, A. (1968) *Arch. Biochem. Biophys. 126*, 232−243.
59. Bairoch, A., and Apweiler, R. (1996) *Nucleic Acids Res. 24*, 21−25.
60. Thompson, J. D., Higgins, D. G., and Gibson, T. J. (1994) *Nucleic Acids Res. 22*, 4673−4680.

BI981016T